

SIMULATION STUDY ON MECHANICAL ADAPTATION IN CANCELLOUS BONE BY TRABECULAR SURFACE REMODELING

Taiji ADACHI,^{*} Ken-ichi TSUBOTA,[†] and Yoshihiro TOMITA[#]

Graduate School of Science and Technology, Kobe University
1-1 Rokkodai, Nada, Kobe 657-8501, Japan

RIKEN
2-1 Hirosawa, Wako-shi, Saitama 351-0198, Japan

^{*} e-mail: adachi@mech.kobe-u.ac.jp

[†] e-mail: tsubota@solid.mech.kobe-u.ac.jp

[#] e-mail: tomita@mech.kobe-u.ac.jp

Abstract. *The relationship between a local mechanical stimulus and trabecular structural change due to osteoclastic/osteoblastic activities was investigated by a trabecular surface remodeling simulation, using a large-scale pixel-based finite element model of the human proximal femur under multiple loadings. In the remodeling rate equation based on the uniform stress hypothesis, the stress/strain at the trabecular level was directly related to the movement of the trabecular surface. As the result of a trabecular structural change toward a local uniform stress state, the apparent bone density distribution and anisotropy of the trabecular microstructure emerged according to the applied external loads. The structural properties at the cancellous bone level corresponded to the mechanical environment evaluated by the apparent principal stress and strain energy. The results of these studies show that the proposed simulation method could provide insight into the macroscopic adaptive phenomenon in cancellous bone resulting from local regulation of the mechanical environment at the trabecular level by cellular activities.*

1. INTRODUCTION

To clarify the mechanism for functional adaptation by mechanical bone remodeling, many phenomenological models (Cowin, 1993) have been proposed based on experimental observations (Goodship *et al.*, 1979; Rubin and Lanyon, 1984; Lanyon, 1987). However, bone remodeling phenomena *in vivo* are very complicated because many mechanical and biological factors are closely linked and influence each other. This makes it difficult to find the quantitative relationship between a mechanical stimulus as a remodeling driving force and bone resorption/formation by local cellular activities. The computational mechanics approach has been used to examine the role of mechanical factors in the bone remodeling phenomenon (Huiskes and Hollister, 1993; Prendergast, 1997). Recent experimental studies (Goldstein *et al.*, 1991; Guldborg *et al.*, 1997) have suggested that a local mechanical stimulus (Cowin *et al.*, 1991) plays an important role in osteoclastic/osteoblastic activities, so the mathematical models for bone remodeling and its simulation method have been refined from the macroscopic ones

based on continuum mechanics (Hart *et al.*, 1984; Cowin *et al.*, 1985; Carter *et al.*, 1987; Huijskes *et al.*, 1987; Carter *et al.*, 1989; Weinans *et al.*, 1992; Van Rietbergen *et al.*, 1993; Jacobs *et al.*, 1997) to the microscopic models (Sadegh *et al.*, 1993; Mullender *et al.*, 1994; Adachi *et al.*, 1997; Adachi *et al.*, 1999a) in which the relationship between a mechanical stimulus and bone morphological change is considered at the trabecular level.

In the present study, trabecular surface remodeling simulation with a large-scale pixel-based finite element model is performed for human proximal femur under multiple loadings to investigate the relationship between a local mechanical stimulus and trabecular structural change due to osteoclastic/osteoblastic activities. In the remodeling rate equation (Adachi *et al.*, 1997) based on the uniform stress hypothesis (Fung, 1984; Takamizawa and Hayashi, 1987; Adachi *et al.*, 1998), the stress/strain at the trabecular level is directly related to the movement of the trabecular surface. Trabeculae in the whole cancellous region are composed of a large number of pixel-based finite elements in the computational simulation, and a trabecular morphological change is accomplished by removing and adding elements. Through a comparison between the structural properties and the mechanical environment evaluated by the apparent principal stress and strain energy in proximal femur, functional adaptation in cancellous bone by local regulation of the mechanical stimulus is discussed.

2. METHODS

2.1 Model for Trabecular Surface Remodeling

Coupled bone resorption and formation occur on the surface of each trabecula in cancellous bone, by a process of successive cellular activities which is called remodeling turnover (Parfitt, 1994). The relative difference between resorption and formation causes apparent movement of the trabecular surface. Considering that a local mechanical stimulus is important to cellular bone remodeling activities, the local quantity of positive scalar function σ of the stress is used as the mechanical stimulus for remodeling (Adachi *et al.*, 1997). Furthermore, by taking account of the hypothesis that a mechanical stimulus becomes uniform at the point of remodeling equilibrium (Fung, 1984; Takamizawa and Hayashi, 1987; Adachi *et al.*, 1998), local nonuniformity of positive scalar function σ of the stress is assumed to be the driving force for trabecular surface remodeling to seek a uniform stress state (Adachi *et al.*, 1997).

Considering that there is a network for intercellular communication (Donahue *et al.*, 1995), the local stress nonuniformity on a trabecular surface is evaluated by using an integral form. Let σ_c denote the stress at point \mathbf{x}_c on the trabecular surface and σ_d denote the representative stress in the area around point \mathbf{x}_c as shown in Fig. 1(a). The local stress nonuniformity at point \mathbf{x}_c is evaluated by the relative value of σ_c to σ_d as follows:

$$\Gamma = \ln(\sigma_c / \sigma_d). \quad (1)$$

Representative stress σ_d is defined by

$$\sigma_d = \int_S w(l) \sigma_r dS / \int_S w(l) dS, \quad (2)$$

where S denotes the trabecular surface, σ_r the stress at point \mathbf{x}_r on the trabecular surface, l the distance between points \mathbf{x}_c and \mathbf{x}_r , and $w(l)$ [$w(l) > 0$ ($0 \leq l < l_L$)] is a weight function depending on distance l . Sensing distance l_L in Fig. 1(a) is a model parameter representing

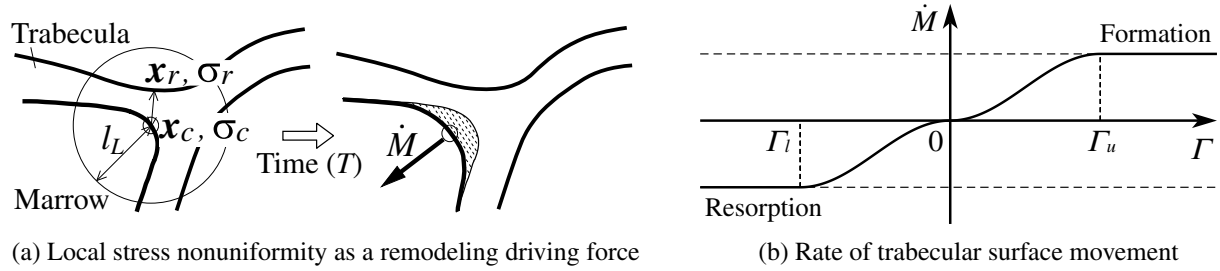


Fig. 1 Model for trabecular surface remodeling based on the uniform stress hypothesis.

the area where cells can sense a mechanical stimulus (Tsubota *et al.*, 2000).

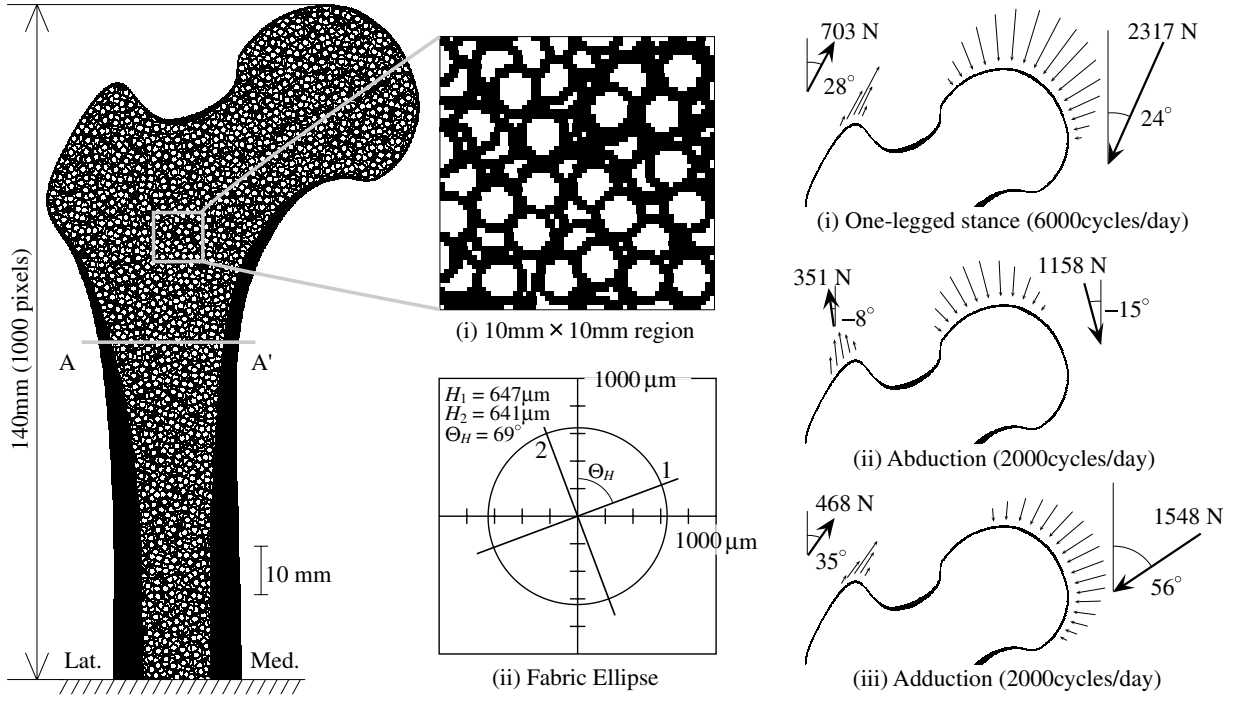
By regarding local stress nonuniformity Γ as the driving force for trabecular surface remodeling, the rate of surface movement is determined as a function of Γ . In general, the surface stress of a load-bearing structure is decreased by adding material to the surface, and increased by its removal. To express the remodeling to seek a local uniform stress state, we define the rate of surface movement \dot{M} , as $\dot{M} > 0$ for the driving force $\Gamma > 0$ and $\dot{M} < 0$ for $\Gamma < 0$, by using the continuous function shown in Fig. 1(b) (Adachi *et al.*, 1997). Model parameters Γ_u and Γ_l in Fig. 1(b) are threshold values of the lazy zone around the remodeling equilibrium point which express the sensitivity of the cells to a mechanical stimulus in time (Tsubota *et al.*, 2000).

2.2 Large-Scale Pixel-Based Finite Element Model of the Proximal Femur

The computational model of the human proximal femur was created with pixel-based finite elements as shown in Fig. 2(a). Assuming an isotropic trabecular structure at the initial stage, the cancellous bone morphology was created by randomly pasting circular trabeculae, as shown in Fig. 2(b), whose external and internal diameters were $1680\mu\text{m}$ and $1120\mu\text{m}$, respectively. The principal values for the fabric ellipse (Cowin, 1985), H_i ($i=1, 2, H_1 > H_2$), of cancellous bone were $H_1 = 647\mu\text{m}$, and $H_2 = 641\mu\text{m}$. The degree of structural anisotropy, H_1/H_2 , was 1.01, indicating that the initial trabecular structure was isotropic. The structural indices for cancellous bone (Feldkamp *et al.*, 1989) were bone volume fraction $BVF = 0.58$, trabecular plate thickness $TPT = 398\mu\text{m}$, trabecular plate number $TPN = 1.47\text{ mm}^{-1}$, trabecular plate separation $TPS = 283\mu\text{m}$, and connectivity $CON = 1.22\text{ mm}^{-2}$.

As the boundary condition to represent the daily loading history applied to the proximal femur in different directions with a differing magnitude of external loading, the multiple-loading condition (Beaupré *et al.*, 1990) shown in Fig. 2(c) was assumed. This loading condition consists of (i) the case of a one-legged stance, (ii) extreme ranges of motion of abduction and (iii) adduction. These external loadings were applied as distributed forces generated by using a sine function to the joint surface and greater trochanter, the lower boundary corresponding to the diaphysis being fixed. Considering that the effect of this lower fixed boundary on the simulation results was small enough to be neglected in the region distant from the boundary, only the proximal region of the model above line A-A' shown in Fig. 2(a) was discussed. The whole area was discretized by 1000 pixel elements in the longitudinal direction and by 553 elements in the horizontal direction, each pixel size being $140\mu\text{m}$. The number of bone elements in the model at the initial stage was 166,106.

The following procedures were conducted for the remodeling simulation with the pixel-based finite element model.



(a) Large scale pixel-based FE model (b) Initial morphology of cancellous bone (c) Boundary condition (Beaupré *et al.*, 1990)

Fig. 2 Computational simulation model for trabecular surface remodeling in the proximal femur

- (1) For loading cases (i), (ii) and (iii), the stress was analyzed by the finite element method with the EBE/PCG approach (Hughes *et al.*, 1987; Van Rietbergen *et al.*, 1995), in which the bone was assumed to be a homogeneous and isotropic material with Young's modulus $E = 20\text{GPa}$ and Poisson's ratio $\nu = 0.3$, and the marrow was not considered as a cavity. The two-dimensional stress analysis carried the assumption of the plane strain condition with a 10mm thickness.
- (2) Representative stress σ_d in Eq.(2) was calculated for each element on the trabecular surface. For simplification, a linearly decreasing function depending on distance l was used for weight function $w(l)$, that is,

$$w(l) = \begin{cases} 1-l/l_L & (0 \leq l \leq l_L) \\ 0 & (l_L \leq l) \end{cases} \quad (3)$$
- (3) Remodeling driving forces Γ_i , Γ_{ii} and Γ_{iii} for loading cases (i), (ii) and (iii) were each calculated from Eq. (1). Driving force Γ for the multiple-loading condition was determined by averaging Γ_i , Γ_{ii} and Γ_{iii} with the weighting depending on the loading frequency (Beaupré *et al.*, 1990).
- (4) Trabecular surface movement determined by Γ , as shown in Fig.1(b), was accomplished by removing and adding trabecular surface elements. To compensate for discretization of the continuous rate of surface movement $\dot{M}(\Gamma)$, probability function $P_M(\Gamma)$ similar to the function in Fig.1(b) was used for removing and adding the surface elements.
- (5) The procedures (1) to (4) were repeated until remodeling equilibrium was attained.

Mises stress was used for stress σ as the mechanical stimulus that cells can sense on the trabecular surface. The series of the procedures (1) to (5) is called one step of the simulation.

3 RESULTS

3.1 Trabecular Structural Change in the Proximal Femur under Multiple Loadings

A trabecular surface remodeling simulation was conducted for cancellous bone in the human proximal femur under multiple loadings from the initial stage up to the 5th step, where the model parameters were set constant as threshold values $\Gamma_u = 1.0$ and $\Gamma_l = -2.0$, and sensing distance $l_L = 1.0\text{mm}$. Nonuniform stress on the trabecular surface induced bone resorption and formation, and resulted in change from the random trabecular architecture at the initial stage, as shown in Fig.2(a), to anisotropic trabecular architecture at the 5th step, as shown in Fig.3(a). The remodeling simulation was continued from the 5th step to the 15th step as shown in Fig.3(b), where the trabecular bone volume was kept constant by changing threshold values Γ_u and Γ_l in order to control the amount of bone formation and resorption for each simulation step, assuming homeostatic state with respect to the amount of trabecular bone. As a result, a higher density region such as H and lower density region such as L were obtained as shown in Fig.3(b), while the characteristic trabecular structure clearly emerged.

In the femoral head represented by region 1, trabeculae were aligned with the compressive joint reaction force. The principal direction of the fabric ellipse was $\Theta_H = 26^\circ$ and the degree of anisotropy was $H_1/H_3 = 1.36$ as shown in Fig.4(a). In the greater trochanter represented by region 2, the trabeculae were aligned with the tensile abductor force. The principal direction of the fabric ellipse was $\Theta_H = 14^\circ$ and the degree of anisotropy was $H_1/H_3 = 1.51$ as shown in Fig.4(b). On the other hand, in the lower region of the neck of the femoral head represented by region 3, compressive trabeculae formed from the medial side to the lateral near the greater trochanter, and tensile trabeculae formed from the lateral to the neck of the femoral head, forming the orthogonal trabecular pattern. The principal direction of the fabric ellipse was $\Theta_H = 24^\circ$ and the degree of anisotropy was $H_1/H_3 = 1.01$ as shown in Fig.4(c).

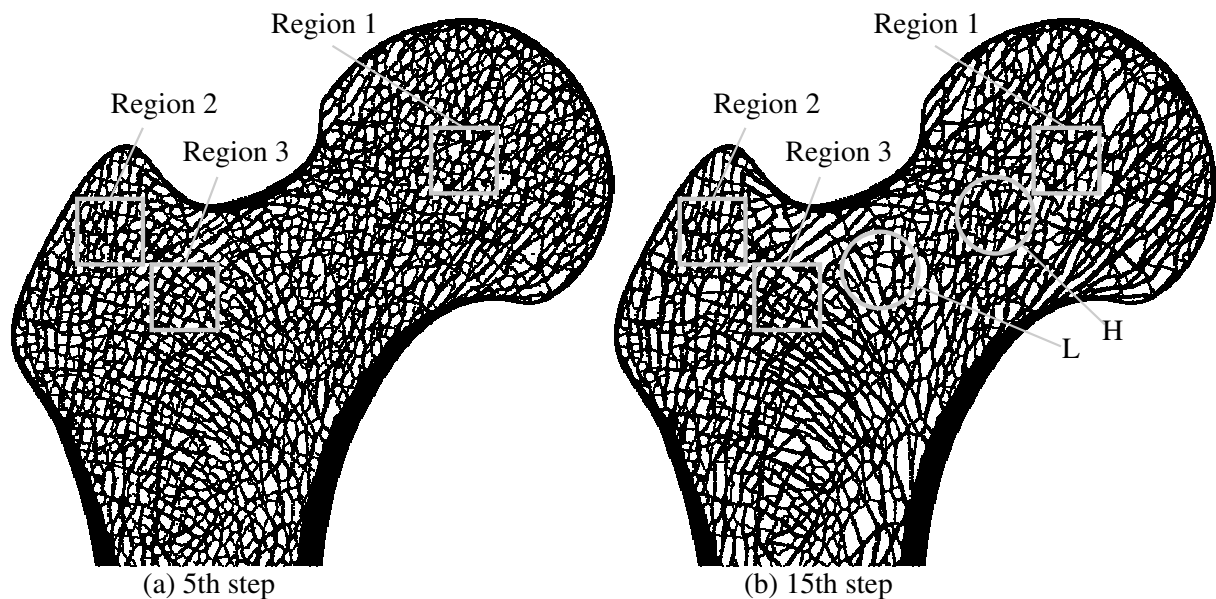


Fig. 3 Trabecular structural change in the proximal femur due to remodeling under multiple loadings

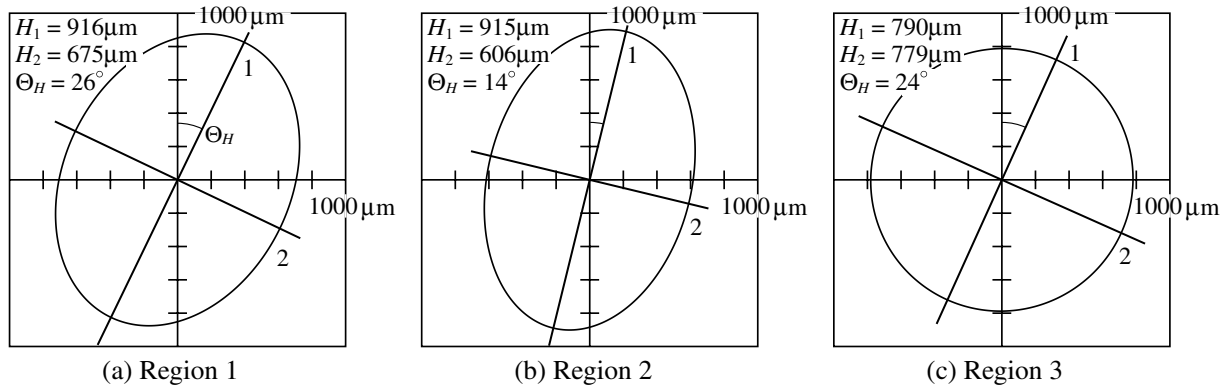


Fig. 4 Fabric ellipses for the cancellous bone in regions 1~3 at 15th step

3.2 Mechanical Adaptation of the Trabecular Structure Due to Remodeling

To investigate the functional adaptation phenomenon in cancellous bone, the change in mechanical environment in the cancellous bone was investigated. Averaging the stress components over the cancellous area for all the loading cases, with the weighting depending on the loading frequency as shown in Fig. 2(c), the apparent principal stress in regions 1~3 at the initial stage and the 15th step was calculated as shown in Fig. 5. The principal stress is subsequently defined as $|\sigma_1| > |\sigma_2|$. At the initial stage, the ratio of the magnitude of two principal stresses, $|\sigma_1|/|\sigma_2|$, was large in regions 1 ($|\sigma_1|/|\sigma_2| = 7.9$) and 2 ($|\sigma_1|/|\sigma_2| = 10.6$), as shown in Fig. 5(a), where a unidirectional trabecular pattern appeared. Therefore, the mechanical environment was almost a uniaxial compressive state in region 1 and a uniaxial

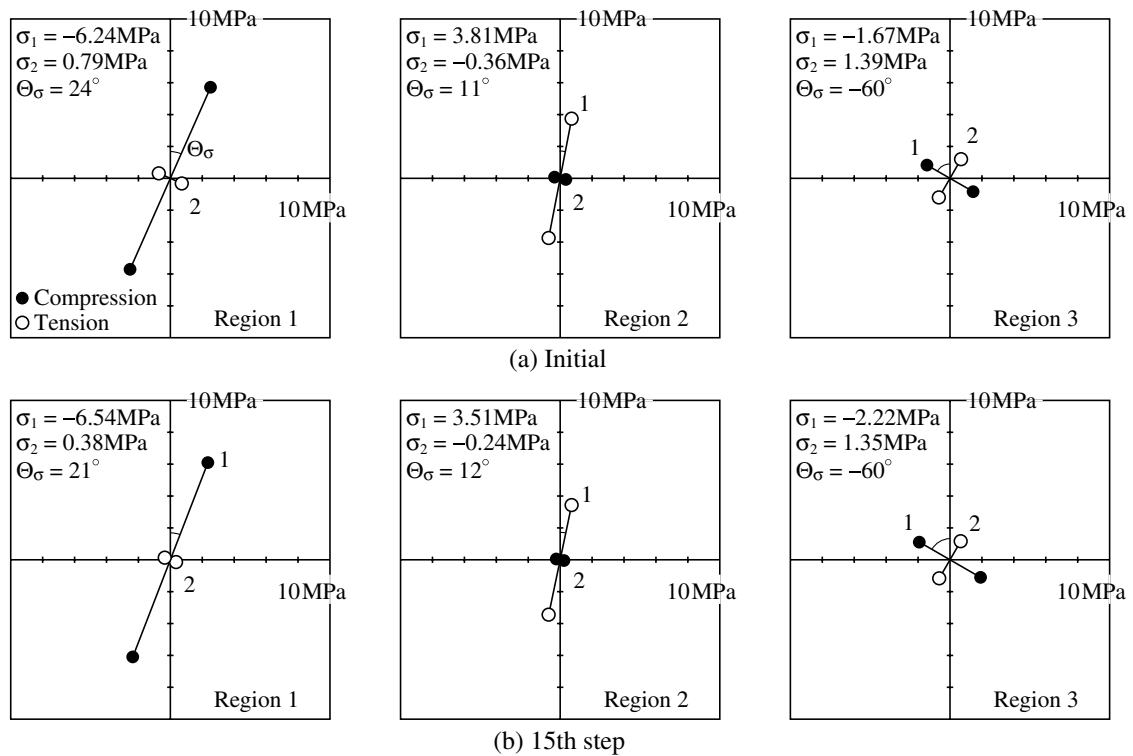


Fig. 5 Apparent principal stress in the cancellous bone in regions 1~3

tensile state in region 2. The principal direction was $\Theta_\sigma = 24^\circ$ in region 1 and $\Theta_\sigma = 11^\circ$ in region 2. In region 3, where the orthogonal trabecular pattern appeared, ratio $|\sigma_1|/|\sigma_2|$ was relatively close to unity ($|\sigma_1|/|\sigma_2| = 1.2$), which means that the mechanical environment was a bi-axial compressive-tensile state. The principal direction was $\Theta_\sigma = -60^\circ$. Although the trabecular structure was changed by remodeling, the two principal stresses, $|\sigma_1|$ and $|\sigma_2|$, and direction Θ_σ at the 15th step, as shown in Fig.5(b), hardly changed from the values at the initial stage.

Averaging the strain energy density over the cancellous region for all the loading cases, with the weighting depending on the loading frequency, change in apparent strain energy density U for regions 1~3 and for the whole bone including the cancellous and cortical sections was calculated as shown in Fig.6. From the initial stage to the 5th step, apparent strain energy density U increased in regions 1 and 3. This shows that the stiffness of the trabecular bone as a load-bearing structure decreased due to the volumetric decrease of the bone. In region 2, however, apparent strain energy density U decreased because the stiffness of the structure increased due to trabecular adaptive reorientation corresponding to the applied external loads. Strain energy density U was found from these results to have changed depending on the degree of both volumetric change and structural reorientation in the trabecular bone. In the whole region, apparent strain energy density U increased to the 5th step, which indicates that the effect of the decrease in bone volume on the stiffness was larger than the effect of the trabecular adaptive reorientation. From the 5th step to the 15th step, by controlling trabecular bone volume to be constant, apparent strain energy density U tended to decrease in regions 1~3 and in the whole bone, where the effect of only trabecular reorientation on the stiffness emerged, and resulted in an increase in the stiffness of cancellous bone as a load-bearing structure.

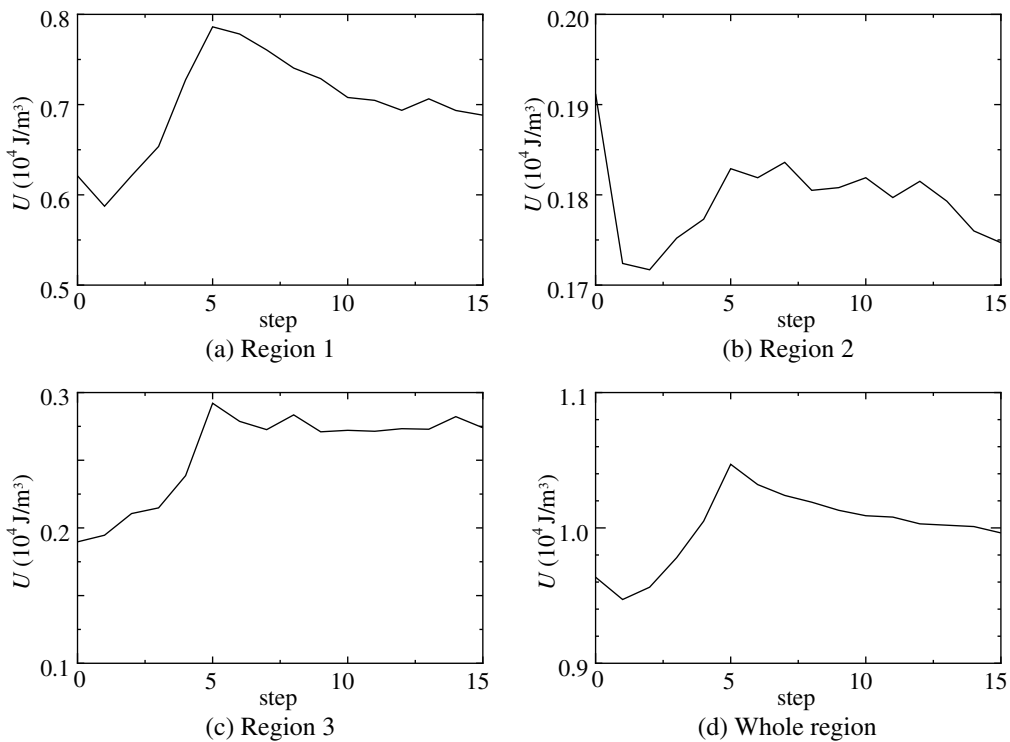


Fig. 6 Change in strain energy density in regions 1~3 and in the whole bone

4 DISCUSSIONS AND CONCLUSION

An anisotropic structure of trabecular bone was obtained according to the mechanical environment in the proximal femur by trabecular surface remodeling to seek a uniform stress state. The effect of loading case (i) on the trabecular structural change was the largest of the three loading cases in this simulation because case (i) was the most frequent. Thus, the obtained trabecular architecture was similar to that obtained under single loading in the case (i) (Adachi *et al.*, 1999b). The trabecular structure, however, was reorganized to adapt to the changed mechanical environment due to multiple loadings, which resulted in a distributed trabecular orientation to some extent.

The principal direction of the fabric ellipse approximately agreed with that of the principal stress, and the degree of anisotropy of the trabecular structure corresponded to the ratio of magnitude of the two principal stresses. Furthermore, it was shown that trabecular reorientation contributed to the increase in stiffness of the trabecular structure in both local regions and in the whole bone. These results indicate that this simulation could well express Wolff's Law (Wolff, 1869) and the functional adaptation phenomenon (Roux, 1881). The predicted distribution of apparent bone density also agrees with the trabecular architecture in the actual proximal femur, for example, the lower bone density region marked by open circle H in Fig.3(b) corresponds to the characteristic trabecular architecture observed in the actual bone (Carter *et al.*, 1989).

It was found that the external-loading conditions affected the equivalent stress distribution of each trabecula in region 1 as shown in Fig.7, which illustrates the ability of a large-scale pixel-based finite element model to predict in detail the influence of external loading on trabecular-level mechanical environment. This point is advantageous in examining the role of osteocytes in trabecular remodeling by integrating over volume element dV in Eq.(2).

The proposed simulation method could provide insight into the macroscopic adaptive phenomenon in cancellous bone resulting from local regulation of the mechanical environment at a trabecular level by cellular activities.

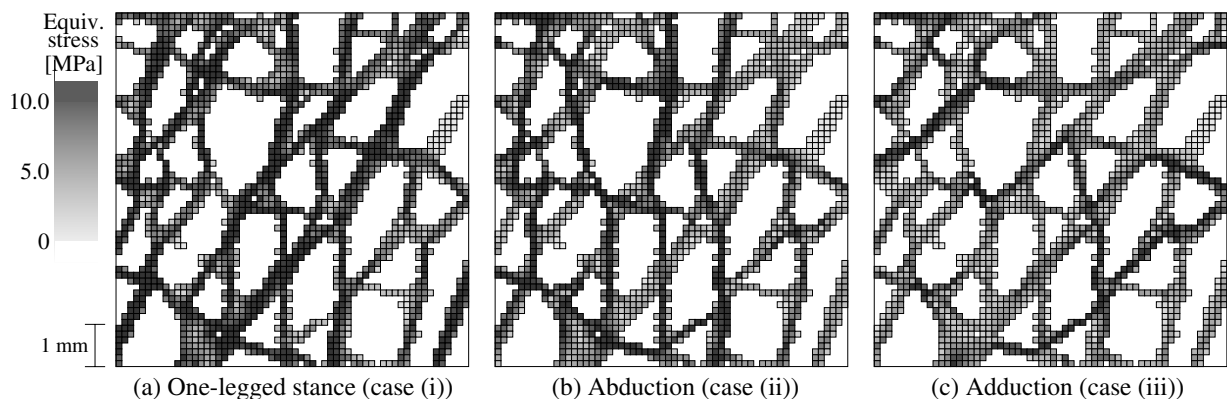


Fig.7 Equivalent stress distribution of each trabecula in region 1 at 15th step under multiple loadings

5 REFERENCES

Adachi, T., Tomita, Y., Sakaue, H., and Tanaka, M. (1997), Simulation of Trabecular Surface Remodeling Based on Local Stress Nonuniformity, *JSME Int. J.*, Vol. 40C, No. 4, pp.

782-792.

- Adachi, T., Tanaka, M., and Tomita, Y. (1998), Uniform Stress State in Bone Structure with Residual Stress, *Trans. ASME, J. Biomech. Eng.*, Vol. 120, No. 3, pp. 342-347.
- Adachi, T., Tomita, Y., and Tanaka, M. (1999a), Three-Dimensional Lattice Continuum Model of Cancellous Bone for Structural and Remodeling Simulation, *JSME Int. J.*, Vol. 42C, No. 3, pp. 470-480.
- Adachi, T., Tsubota, K., and Tomita, Y. (1999b), Computational Simulation of Mechanical Adaptation in Cancellous Bone by Trabecular Surface Remodeling, *J. Jpn. Soc. Simul. Tech.*, Vol. 18, No. 4, pp. 251-259 (in Japanese).
- Beaupré, G. S., Orr, T. E., and Carter, D. R. (1990), An Approach for Time-Dependent Bone Modeling and Remodeling – Application: A Preliminary Remodeling Simulation, *J. Orthop. Res.*, Vol. 8, pp. 662-670.
- Carter, D. R., Fyhrie, D. P., and Whalen, R. T. (1987), Trabecular Bone Density and Loading History: Regulation of Connective Tissue Biology by Mechanical Energy, *J. Biomech.*, Vol. 20, No. 8, pp. 785-794.
- Carter, D. R., Orr, T. E., and Fyhrie, D. P. (1989), Relationships between Loading History and Femoral Cancellous Bone Architecture, *J. Biomech.*, Vol. 22, No. 3, pp. 231-244.
- Cowin, S. C. (1985), The Relationship between the Elasticity Tensor and the Fabric Tensor, *Mechanics of Materials*, Vol. 4, pp. 137-147.
- Cowin, S. C., Hart, R. T., Balser, J. R., and Kohn, D. H. (1985), Functional Adaptation in Long Bones: Establishing *in Vivo* Values for Surface Remodeling Rate Coefficients, *J. Biomech.*, Vol. 18, No. 9, pp. 665-684.
- Cowin, S. C., Moss-Salentijn, L., and Moss, M. L. (1991), Candidates for the Mechanosensory System in Bone, *Trans. ASME, J. Biomech. Eng.*, Vol. 113, No. 2, pp. 191-197.
- Cowin, S. C. (1993), Bone Stress Adaptation Models, *Trans. ASME, J. Biomech. Eng.*, Vol. 115, No. 4B, pp. 528-533.
- Donahue, H. J., McLeod, K. J., Rubin, C. T., Andersen, J., Grine, E. A., Hertzberg, E. L., and Brink, P. R. (1995), Cell-to-Cell Communication in Osteoblastic Networks: Cell Line-Dependent Homonal Regulation of Gap Junction Function, *J. Bone & Mineral Res.*, Vol. 10, No. 6, pp. 881-889.
- Feldkamp, L. A., Goldstein, S. A., Parfitt, A. M., Jesion, G., and Kleerekoper, M. (1989), The Direct Examination of Three-Dimensional Bone Architecture In Vitro by Computed Tomography, *J. Bone & Mineral Res.*, Vol. 4, No. 1, pp. 3-11.
- Fung, Y. C. (1984), In *Biodynamics: Circulation*, pp. 64, Springer.
- Goldstein, S. A., Matthews, L. S., Kuhn, J. L., and Hollister, S. J. (1991), Trabecular Bone Remodeling: An Experimental Model, *J. Biomech.*, Vol. 24, Suppl. 1, pp. 135-150.
- Goodship, A. E., Lanyon, L. E., and McFie, H. (1979), Functional Adaptation of Bone to Increased Stress: An Experimental Study, *J. Bone Jt. Surg.*, Vol. 61A, No. 4, pp. 539-546.
- Guldberg, R. E., Richards, M., Caldwell, N. J., Kuelske, C. L., and Goldstein, S. A. (1997), Trabecular Bone Adaptation to Variations in Porous-Coated Implant Topology, *J. Biomech.*, Vol. 30, No. 2, pp. 147-153.
- Hart, R. T., Davy, D. T., and Heiple, K. G. (1984), A Computational Method for Stress Analysis of Adaptive Elastic Materials with a View toward Applications in Strain-Induced Bone Remodeling, *Trans. ASME, J. Biomech. Eng.*, Vol. 106, No. 4, pp. 342-350.
- Hughes, T. J. R., Ferencz, R. M., and Hallquist, J. O. (1987), Large-Scale Vectorized Implicit

- Calculations in Solid Mechanics on a Cray X-MP/48 Utilizing EBE Preconditioned Conjugate Gradients, *Comp. Methods Appl. Mech. Eng.*, Vol. 61, pp. 215-248.
- Huiskes, R., Weinans, H., Grootenboer, H. J., Dalstra, M., Fudala, B., and Slooff, T. F. (1987), Adaptive Bone-Remodeling Theory Applied to Prosthetic-Design Analysis, *J. Biomech.*, Vol. 20, No. 11/12, pp. 1135-1150.
- Huiskes, R., and Hollister, S. J. (1993), From Structure to Process, From Organ to Cell: Recent Developments of FE-Analysis in Orthopaedic Biomechanics, *Trans. ASME, J. Biomech. Eng.*, Vol. 115, No. 4B, pp. 520-527.
- Jacobs, C. R., Simo, J. C., Beaupré, G. S., and Carter, D. R. (1997), Adaptive Bone Remodeling Incorporating Simultaneous Density and Anisotropy Considerations, *J. Biomech.*, Vol. 30, No. 6, pp. 603-613.
- Lanyon, L. E. (1987), Functional Strain in Bone Tissue as an Objective, and Controlling Stimulus for Adaptive Bone Remodeling, *J. Biomech.*, Vol. 20, No. 11/12, pp. 1083-1093.
- Mullender, M. G., Huiskes, R., and Weinans, H. (1994), A Physiological Approach to the Simulation of Bone Remodeling as a Self Organization Control Process, *J. Biomech.*, Vol. 27, No. 11, pp. 1389-1394.
- Parfitt, A. M. (1994), Osteonal and Hemi-Osteonal Remodeling: The Spatial and Temporal Framework for Signal Traffic in Adult Human Bone, *J. Cellular Biochem.*, Vol. 55, pp. 273-286.
- Prendergast, P. J. (1997), Finite Element Models in Tissue Mechanics and Orthopaedic Implant Design, *Clin. Biomech.*, Vol. 12, No. 6, pp. 343-366.
- Roux, W. (1881), Der Züchtende Kampf der Teil, Oder die 'Teilauslese' im Organismus (Theorie der 'Funktionellen Anpassung'), Wilhelm Engelmann.
- Rubin, C. T., and Lanyon, L. E. (1984), Regulation of Bone Formation by Applied Dynamic Loads, *J. Bone Jt. Surg.*, Vol. 66A, No. 3, pp. 397-402.
- Sadegh, A. M., Luo, G. M., and Cowin, S. C. (1993), Bone Ingrowth: An Application of the Boundary Element Method to Bone Remodeling at the Implant Interface, *J. Biomech.*, Vol. 26, No. 2, pp. 167-182.
- Takamizawa, K., and Hayashi, K. (1987), Strain Energy Density Function and Uniform Strain Hypothesis for Arterial Mechanics, *J. Biomech.*, Vol. 20, No. 1, pp. 7-17.
- Tsubota, K., Adachi, T., and Tomita, Y. (2000), Simulation Study on Model Parameters of Trabecular Surface Remodeling Model, In *Proc. 4th Int. Symp. on Comp. Meth. in Biomech. & Biomed. Eng.* (in press).
- Van Rietbergen, B., Huiskes, R., Weinans, H., Sumner, D. R., Turner, T. M., and Galante, J. O. (1993), The Mechanism of Bone Remodeling and Resorption around Press-Fitted THA Stems, *J. Biomech.*, Vol. 26, No. 4/5, pp. 369-382.
- Van Rietbergen, B., Weinans, H., Huiskes, R., and Odgaard, A. (1995), A New Method to Determine Trabecular Bone Elastic Properties and Loading Using Micromechanical Finite-Element Models, *J. Biomech.*, Vol. 28, No. 1, pp. 69-81.
- Weinans, H., Huiskes, R., and Grootenboer, H. J. (1992), The Behavior of Adaptive Bone-Remodeling Simulation Models, *J. Biomech.*, Vol. 25, No. 12, pp. 1425-1441.
- Wolff, J. (1869), Ueber die Bedeutung der Architectur der Spongiösen Substanz für die Frage vom Knochenwachstum, *Zentralblatt für die Medizinischen Wissenschaften*, Vol. 6, pp. 223-234.